Life Sciences 235 (2019) 116829

Contents lists available at ScienceDirect

Life Sciences

journal homepage: www.elsevier.com/locate/lifescie

LncRNA NEAT1 promotes hepatic lipid accumulation via regulating miR-146a-5p/ROCK1 in nonalcoholic fatty liver disease

Xi Chen, Xin-Rui Tan, Shi-Jun Li, Xing-Xing Zhang*

Department of Pediatrics, The Second Xiangya Hospital, Central South Univeristy, Changsha 410011, Hunan Province, PR China

ARTICLE INFO

Keywords:
NEAT1
miR-146a-5p
ROCK1
NAFLD

ABSTRACT

Background: Nonalcoholic fatty liver disease (NAFLD) is a severe liver disease, which influences the health of people worldwide. However, the specific mechanism of the disease remains unknown, and effective treatments are still lacking. It was reported that Nuclear enriched abundant transcript 1 (NEAT1) obviously was up-regulated in NAFLD model. But the role and underlying mechanism of NEAT1 in NAFLD is unclear.

Methods: HepG2 cells were treated by free fatty acids (FFA) and C57BL/6J mice were treated by high-fat diet to establish NAFLD in vitro and in vivo models, respectively. Cell transfection was applied to regulate the expression of NEAT1, ROCK1, and miR-146a-5p. Western blotting and qRT-PCR were used for measuring expression of protein and mRNA level, respectively. Dual luciferase assay was used to detect the target relationship. Oil Red O staining was used to measure the lipid accumulation. HE staining was used for observing pathological feature of liver tissues.

Results: High levels of NEAT1 and ROCK1, and low level of miR-146a-5p were identified in NAFLD models. NEAT1 could target miR-146a-5p to promote ROCK1 expression. Knockdown of NEAT1, overexpression of miR-146a-5p and knockdown of ROCK1 inhibited lipid accumulation through activating AMPK pathway.

Conclusion: NEAT1 may regulate NAFLD through miR-146a-5p targeting ROCK1, and further affect AMPK/SREBP pathway. This study may provide a new thought for the treatment of NAFLD.

1. Introduction

Liver is the key metabolic organ of the human body, and it plays an important role in maintaining the lipid homeostasis. Dysfunction of liver leads to metabolic disorder of lipid, which is closely linked with diabetes, obesity, and metabolic disease [1,2]. Nonalcoholic fatty liver disease (NAFLD) is a chronic metabolic disorder of the liver, which has emerged as a major public health concern with a high prevalence rate ranging from 12.9% to 46.0% depending on different countries [3,4]. NAFLD contains a histological changes ranging from simple steatosis to nonalcoholic steatohepatitis, advanced fibrosis, cirrhosis and finally liver failure or hepatocellular carcinoma [5]. The pathogenesis of NAFLD is complicated and involved in environmental and genetic factors, hormone secretion, lipid peroxidation damage, immunological reactions, oxidative stress, and abnormal fat metabolism [5–7]. However, these mechanisms are not well understood, and effective methods for preventing and treating NAFLD are still lacking.

Long non coding RNAs (lncRNAs) belong to non-protein-coding RNA, and they play a key role in many human diseases by regulating microRNAs [8–10]. Nuclear enriched abundant transcript 1 (NEAT1), a type of nuclear lncRNA, is essential for the formation of paraspeckles, which participates in oxLDL-induced macrophage inflammation and lipid uptake [11,12]. NEAT1 plays a vital role in adipogenesis such as low-density lipoprotein oxidization, lipid uptake, and lipolysis [13]. Meanwhile, knockdown of NEAT1 alleviated the NAFLD via mTOR/S6K1 pathway, which modulated the biosynthesis of protein and lipid. Suppression of mTOR/S6K1 pathway could reduce the increased FAS and ACC caused by FFA in vitro [11]. MicroRNAs (miRNAs) act as regulators during gene expression and cellular function. The role of miRNAs in many physiological processes has been widely investigated, and they mostly function at the posttranscriptional level [14]. It was reported that microRNA-140 (miR-140) physically interacted with NEAT1 and promoted NEAT1 expression. Therefore, NEAT1 might participate in miR-140-induced adipogenesis and further regulate NAFLD, and the positive regulation of NEAT1 by miR-140 was necessary for adipogenesis [15,16]. Previous reports suggested that miR-146a-5p participated NAFLD pathogenesis by inhibiting proliferation and activation of hepatic stellate cells in nonalcoholic brosing

* Corresponding author at: Department of Pediatrics, The Second Xiangya Hospital, Central South Univeristy, No. 139, Middle Renmin Road, Changsha 410011, Hunan Province, PR China.
E-mail address: zhangxingxing@csu.edu.cn (X.-X. Zhang).

https://doi.org/10.1016/j.lfs.2019.116829
Received 14 May 2019; Received in revised form 26 August 2019; Accepted 31 August 2019
Available online 01 September 2019

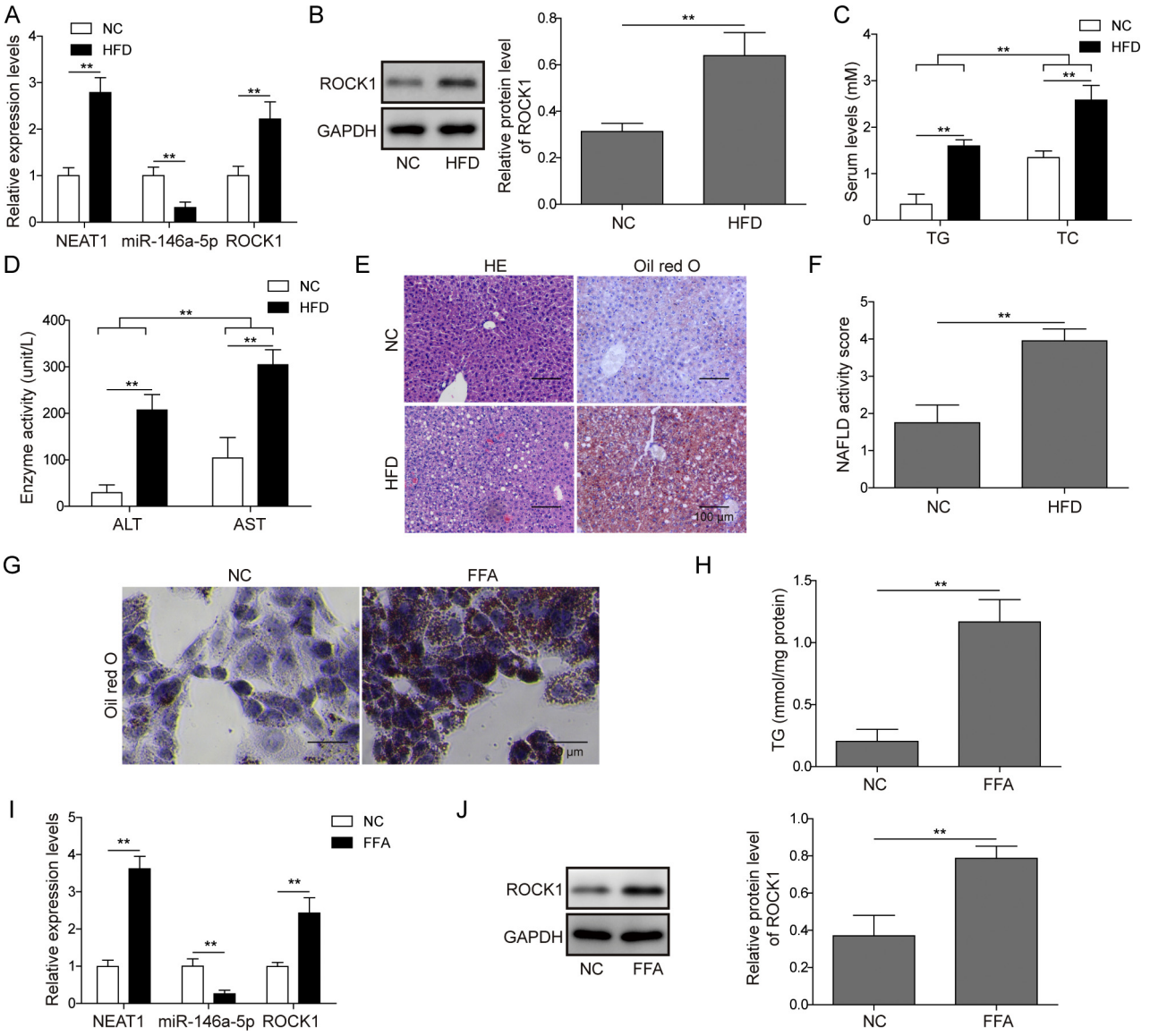

Fig. 1. NEAT1 and ROCK1 were up-regulated and miR-146a-5p was down-regulated in NAFLD models. (A) The relative expression levels of NEAT1, miR-146a-5p, and ROCK1 were measured by qPT-PCR in mice. (B) The protein level of ROCK1 was measured by Western blotting. (C) The content of serum TG and TC in mice. (D) The content of serum ALT and AST in mice. (E) Hepatic steatosis was identified in liver tissues by HE staining, and lipid deposition in liver tissues was detected by Oil Red O staining. (F) NAFLD activity score was quantified after HFD treatment. (G) Intracellular lipid accumulation was observed by Oil Red O staining. (H) The TG level in HepG2 cells. (I) The relative expression levels of NEAT1, miR-146a-5p, and ROCK1 were detected by qPT-PCR in HepG2 cells. (J) The protein level of ROCK1 was detected by Western blotting in HepG2 cells. Data were shown as the mean ± SD. Each experiment was repeated three times. $^{*}P < 0.05$, $^{**}P < 0.01$.

steatohepatitis [17,18]. Meanwhile, we found targeted binding site between NEAT1 and miR-146a-5p by bioinformatics, so we speculated that NEAT1 and miR-146a-5p might function with each other and influence the pathogenesis of NAFLD.

Rho-kinase (ROCK) isoforms, ROCK1 and ROCK2, have been implicated in several physiological activities, including actin cytoskeleton organization, smooth muscle contraction, cell motility and adhesion, and gene expression [1,19,20]. Emerging data demonstrated that ROCK1 was significantly up-regulated in humans with fatty liver disease and linked with risk factors clustering around NAFLD [1]. Meanwhile, overexpression of hepatic ROCK1 could promote the progression of obesity-associated NAFLD, and inhibition of hepatic ROCK1 might be a novel therapeutic target for the treatment of NAFLD [1]. The binding site between miR-146a-5p and ROCK1 was identified by bioinformatics [21], but the regulatory mechanism of them in NAFLD is presently unknown.

In the present study, we established the models of NAFLD both in vivo and in vitro, and the regulation of lipid accumulation in NAFLD by NEAT1/miR-146a-5p/ROCK1 was investigated. This study may provide a novel therapeutic target for the treatment of NAFLD.

2. Materials and methods

2.1. Cell culture and treatment

The HepG2 cells were obtained from the American Type Culture Collection (Manassas, Virginia, USA). The cells were cultured in Dulbecco's Modified Eagle's Medium (DMEM, Gibico, USA) with 10% fetal bovine serum (Invitrogen, Carlsbad, CA, USA) in a humidified atmosphere of 5% CO_2 at 37 °C.

To establish the cell model, HepG2 cells were subjected to 1 mM free fatty acids (FFA, oleate: palmitate = 2:1; Invitrogen, USA) for 24 h and the control cells were maintained in normal DMEM. Then the cells were used for different experiments in this study.

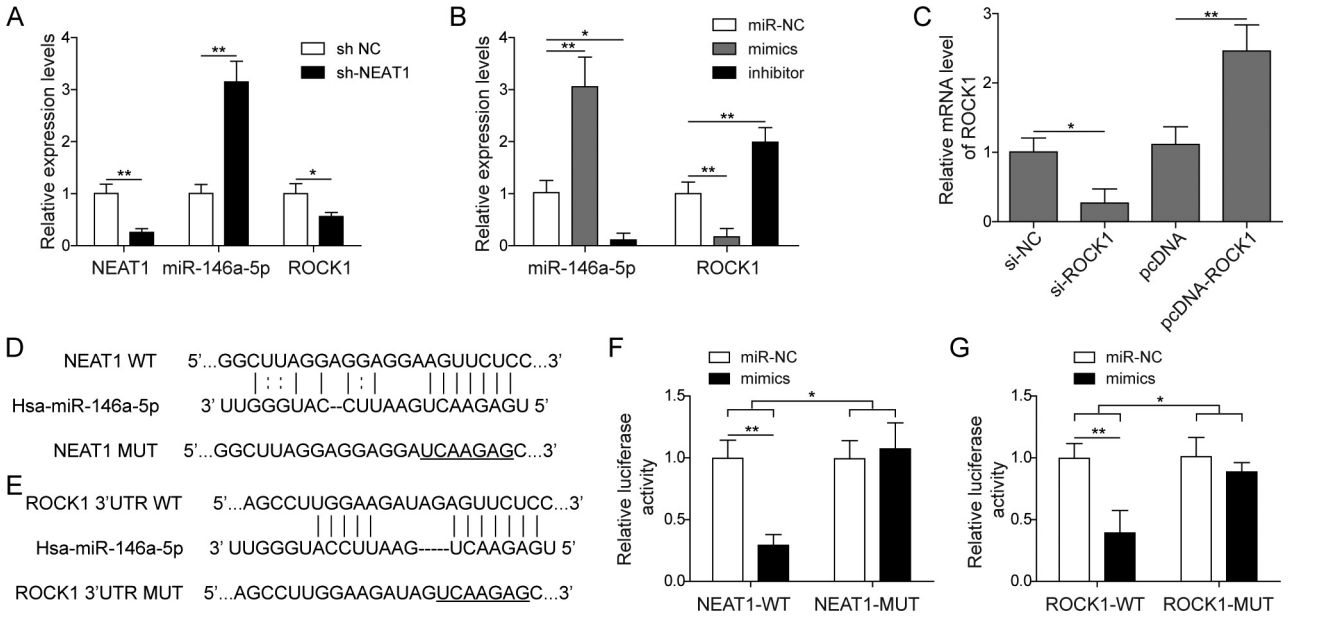

Fig. 2. NEAT1 promoted the expression of ROCK1 via sponging miR-146a-5p. (A) The expression levels of NEAT1, miR-146a-5p and ROCK1 were measured by qRT-PCR in HepG2 cells transfected with sh-NEAT1. (B) The expression levels of miR-146a-5p and ROCK1 were detected by qRT-PCR in HepG2 cells transfected with miR-146a-5p mimics or inhibitor. (C) The expression level of ROCK1 was detected by qRT-PCR in HepG2 cells transfected with si-ROCK1 or pcDNA-ROCK1. (D) Sequence prediction between NEAT1 and miR-146a-5p. (E) Sequence prediction between miR-146a-5p and ROCK1. (F) Relative luciferase activity for binding between NEAT1 and miR-146a-5p. (G) Relative luciferase activity for binding between miR-146a-5p and ROCK1. Data were shown as the mean ± SD. Each experiment was repeated three times. $^{*}P < 0.05$, $^{**}P < 0.01$.

2.2. NAFLD animal model

The animal model was established as described [22,23]. Twelve C57BL/6J mice (gender: male, weight: 22–25 g) were obtained from Beijing Vital River Laboratory Animal Technology (Beijing, China). The animal experiments were approved by experimental animal ethical committee of The Second Xiangya Hospital of Central South University. Animals were randomly divided into normal diet control (NC) group and high-fat diet (HFD) group. All mice were raised with pathogen-free facility and 12 h day and night cycle at 20–26 °C. The mice in NC group were fed with normal diet (65% carbohydrate, 10% fat and 25% protein) and the mice in HFD group were fed with high-fat diet (35% carbohydrate, 50% fat and 15% protein) for 12 weeks. Then mice were sacrificed, blood samples and liver tissues were collected and stored.

2.3. Cell transfection

sh-NEAT1, miR-146a-5p mimics and inhibitor, pcDNA-ROCK1 and si-ROCK1 were all designed and synthesized by GenePharma Co., Ltd. (Shanghai, China). Cells were seeded on 60-mm dishes and cultured for 24 h. After 60% cell confluence was reached, cell transfection and co-transfection were conducted with Lipofectamine 2000 (Invitrogen Life, USA). Lipofectamine 2000 suspension was prepared with 250 μL Opti-MEM and 5 μL Lipofectamine 2000. After incubation with the suspension for 6 h on the condition of 37 °C and 5% CO_2, the transfection efficiency was measured, and medium was replaced. Cells were collected after 48 h incubation at 37 °C in a humidified atmosphere containing 5% CO_2.

2.4. Triglyceride assay

Cells from different groups were collected and washed twice with PBS. The intracellular TG was explored using a triglyceride assay kit (Applygen Technologies, Beijing, China). Each group was repeated three experiments.

2.5. BODIPY-labeled fatty acid uptake assay

The BODIPY-labeled fatty acid uptake assay was applied as described previously [24]. Briefly, HepG2 cells were incubated with 1 μM BODIPY-labeled fatty acid (C16; Invitrogen, USA) for 30 min at 37 °C. Then surface-associated BODI- PY was removed using PBS containing 0.2% BSA at 4 °C. BODIPY fluorescence was measured with SpectraMax i3 fluorescence plate reader (Molecular Devices, Inc., USA).

2.6. HE staining

The liver tissues were collected and stained as described [22,25]. Briefly, the mice were sacrificed and liver tissues were removed using surgical scissors. Then, tissues fixed using 4% paraformaldehyde were used for paraffin embedded slice. Tissue slices were dewaxed in xylene (10 min). Then gradient alcohol was used for dehydrating after washing with distilled water (10 min). Sections were stained by hematoxylin (5 min), differentiated by 1% hydrochloric acid for (30 s), and dyed using 1% eosin-alcohol (5 min). After gradient alcohol dehydration and mounting, a microscope (Olympus, Japan) was used for observation. For quantitative evaluation of hepatic steatosis, NAFLD activity score (NAS), which consists of steatosis, lobular inflammation, and ballooning, was used [26].

2.7. Oil Red O staining

The cells were stained by Oil Red O (Sigma, USA) as described [27]. Briefly, cells were fixed in 10% phosphate buffered formalin (10 min), rinsed in PBS once (1 min), and then rinsed in 50% isopropanol (15 s) to facilitate the staining of neutral lipids. The cells were stained with filtered Oil Red O at 37 °C (1 min) in darkness. Then detain the cells with 60% isopropanol (15 s). Wash cells with PBS for 2 times (5 min each time). Finally, cells were viewed through a microscope (Olympus) and then photographed with Image Pro-Plus 6.0 software (Media Cybernetics, USA).

Slices of tissues were fixed using 10% ice paraformaldehyde for

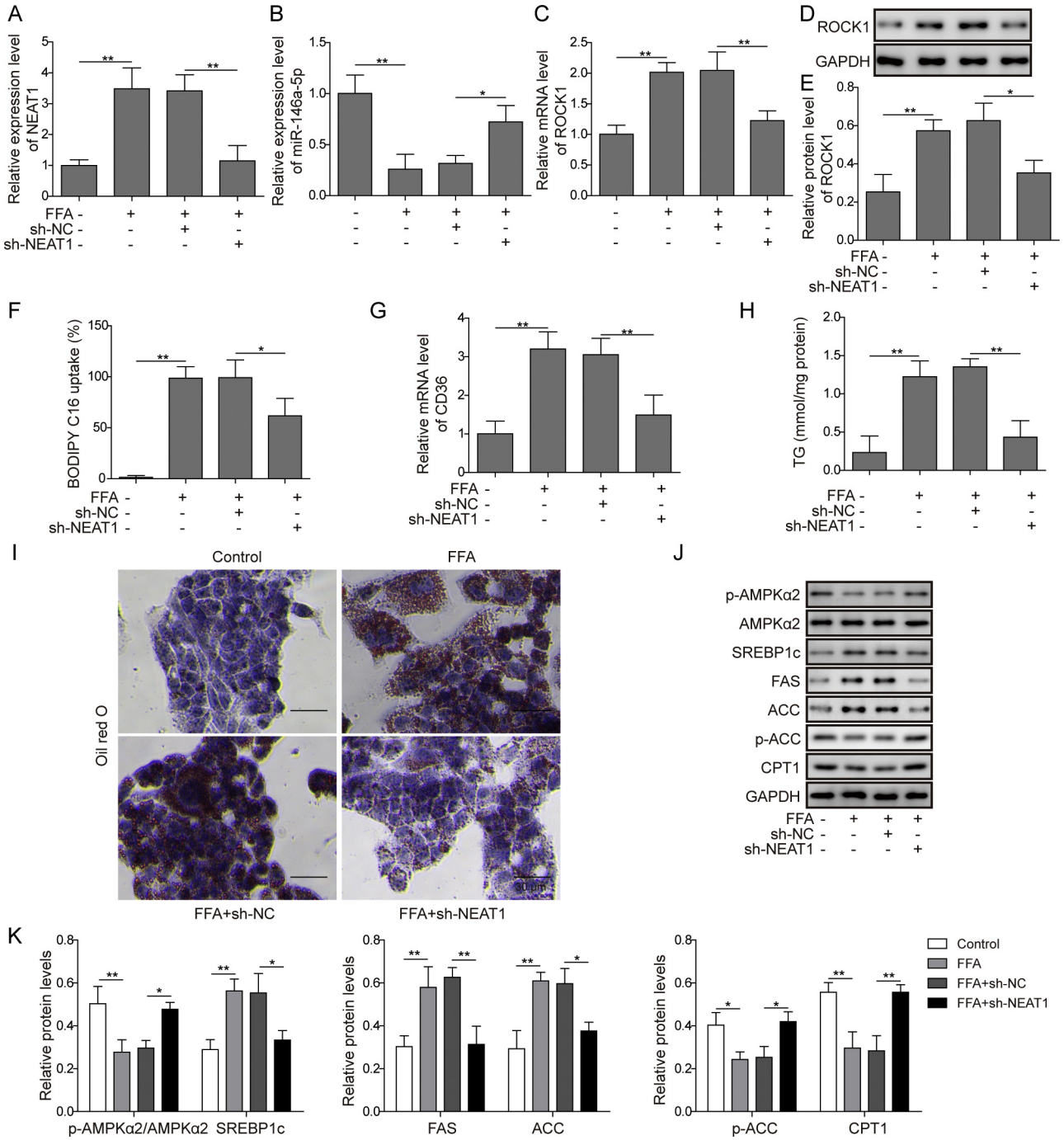

Fig. 3. Down-regulation of NEAT1 remitted lipid formation. (A) The mRNA level of NEAT1 in HepG2 cells transfected with sh-NEAT1. (B) The level of miR-146a-5p in HepG2 cells transfected with sh-NEAT1. (C–E) The protein and mRNA level of ROCK1 in HepG2 cells transfected with sh-NEAT1. (F) The BODIPY C16 uptake in HepG2 cells after transfection with sh-NEAT1. (G) The mRNA level of CD36 in HepG2 cells transfected with sh-NEAT1. (H) The TG level in HepG2 cells transfected with sh-NEAT1. (I) Lipid accumulation in HepG2 cells transfected with sh-NEAT1 identified by Oil Red O staining. (J–K) The protein levels of AMPK/SREBP signaling pathway-related protein were measured by Western blotting in HepG2 cells transfected with sh-NEAT1. Data were shown as the mean ± SD. Each experiment was repeated three times. $^{*}P < 0.05$, $^{**}P < 0.01$.

(10 min), and washed with distilled water for 3 times. After drying (5 min), deionized water and oil red were diluted in a 2:3 ration (10 min). After that, sections experienced Oil Red O staining (5 min), 80% propylene glycol solution differentiation (3 min), washing (2 times), hematoxylin counterstained (30 s), flushed with water (3 min), and mounting.

2.8. Dual luciferase reporter assay

The wild-type fragments from NEAT1 (NEAT1-WT) containing the potential binding sites of miR-146a-5p and corresponding mutant type fragments (NEAT1-MUT) were cloned into pmirGlO vector (Promega, Madison, WI, USA), respectively. Similarly, the WT fragment from the ROCK1 3′-UTR region (ROCK1-WT) and the corresponding MUT fragment (ROCK1-MUT) were cloned into the plasmids of pmirGlO vector to generate the ROCK1 3′-UTR luciferase reporter construct. Then, the

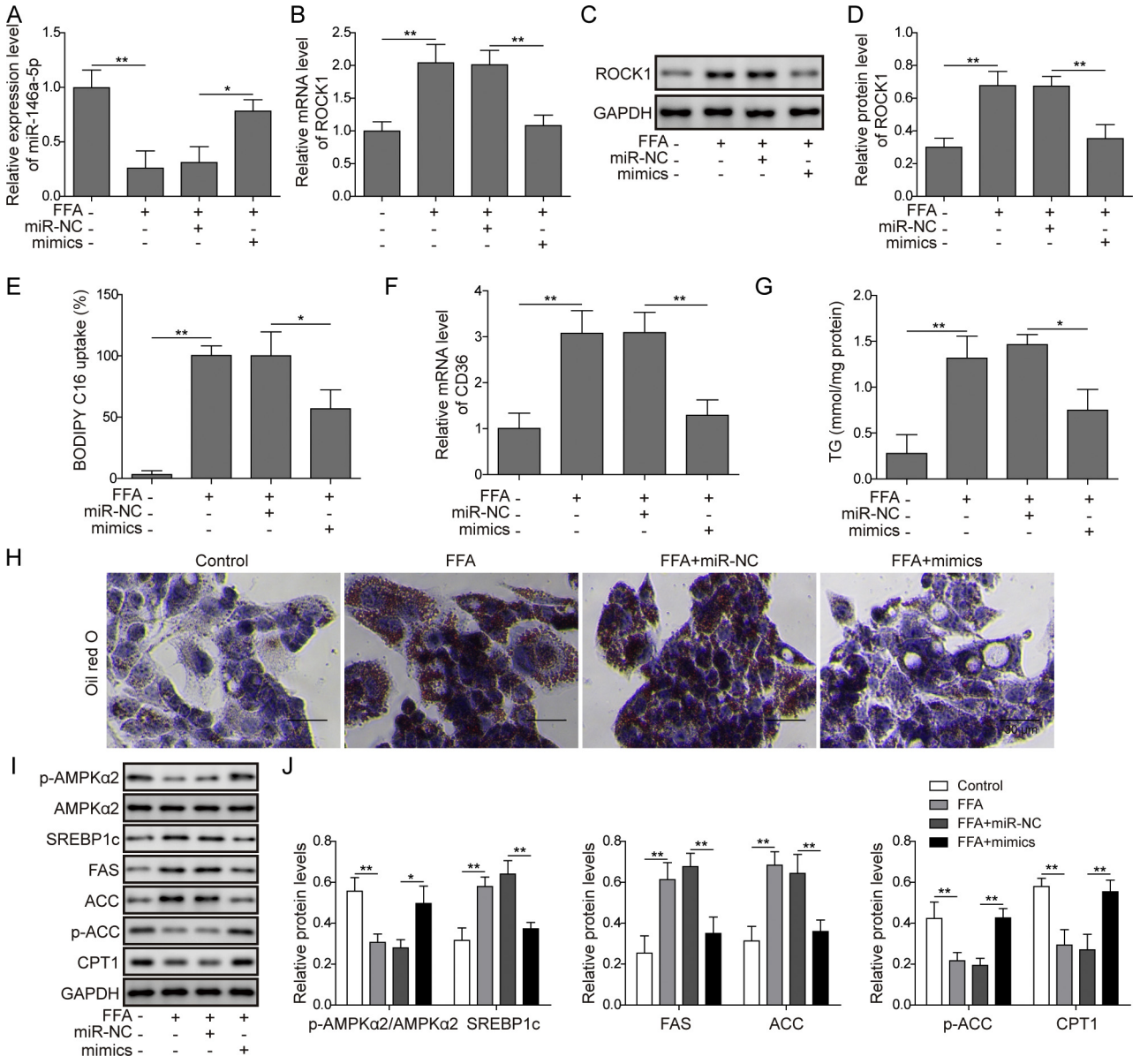

Fig. 4. Overexpression of miR-146a-5p moderated lipid deposition induced by FFA. (A) The level of miR-146a-5p in HepG2 cells transfected with miR-146a-5p mimics. (B–D) The protein and mRNA level of ROCK1 in HepG2 cells transfected with miR-146a-5p mimics. (E) The BODIPY C16 uptake in HepG2 cells transfected with miR-146a-5p mimics. (F) The mRNA level of CD36 in HepG2 cells transfected with miR-146a-5p. (G) The TG content in HepG2 cells transfected with miR-146a-5p mimics. (H) Lipid accumulation in HepG2 cells transfected with miR-146a-5p mimics identified by Oil Red O staining. (I–J) The protein expressions of AMPK/SREBP signaling pathway-related protein were detected by Western blotting in HepG2 cells transfected with miR-146a-5p mimics. Data were shown as the mean ± SD. Each experiment was repeated three times. $^{*}P < 0.05$, $^{**}P < 0.01$.

vectors and miR-146a-5p mimics were co-transfected into HepG2 cells with Lipofectamine 2000 reagent (Invitrogen, USA). Cells were then collected 48 h after transfection and the activities of firefly and Renilla luciferases were detected with the Dual-Luciferase Reporter Assay System (Promega, USA) and standardized those of Renilla luciferase activities.

2.9. Biochemical measurements

Mice were sacrificed after 12 weeks, and blood samples were collected using eye-balls removal method. Then aminotransferase (ALT), aspartate aminotransferase (AST), triglyceride (TG), and total cholesterol (TC) concentrations were detected using an automatic biochemical analyzer 7180 (Hitachi Ltd., Tokyo, Japan).

2.10. RNA extraction and real-time PCR

Total RNA was extracted using TRIzol reagent (Invitrogen, USA) and 500 ng RNA was reverse-transcribed into cDNA using the Primer Script RT reagent kit (Takara Bio, China). Real-time PCR was performed using SYBR Premix Ex TaqTM II kit (Takara Bio, China). The primers were listed as follows: (1) NEAT1: forward: 5′-GCTCTGGGACCTTCGT GACTCT-3′ and reverse: 5′-CTGCCTTGGCTTGGAAATGTAA-3′; (2) miR-146a-5p: forward: 5′-CCGATGTGTATCCTCAGCTTTG-3′ and reverse: 5′-GCCTGAGACTCTGCCTTCTG-3′; (3) ROCK1: forward: 5′-ATGAGTT TATTCCTACACTCTACCACTTTC-3′ and reverse: 5′-TAACATGGCATCT TCGACACTCTAG-3′. (4) GAPDH: forward: 5′-CCACCCATGGCAAATTC CATGGCA-3′ and reverse: 5′-TCTAGACGGCAGGTCAGGTCCACC-3′. (5) U6: forward: 5′-ATTGGAACGATACAGAGAAGATTAG-3′ and reverse: 5′-TGCGTGTCGTGGAGTC-3′. Every sample was replicated three times

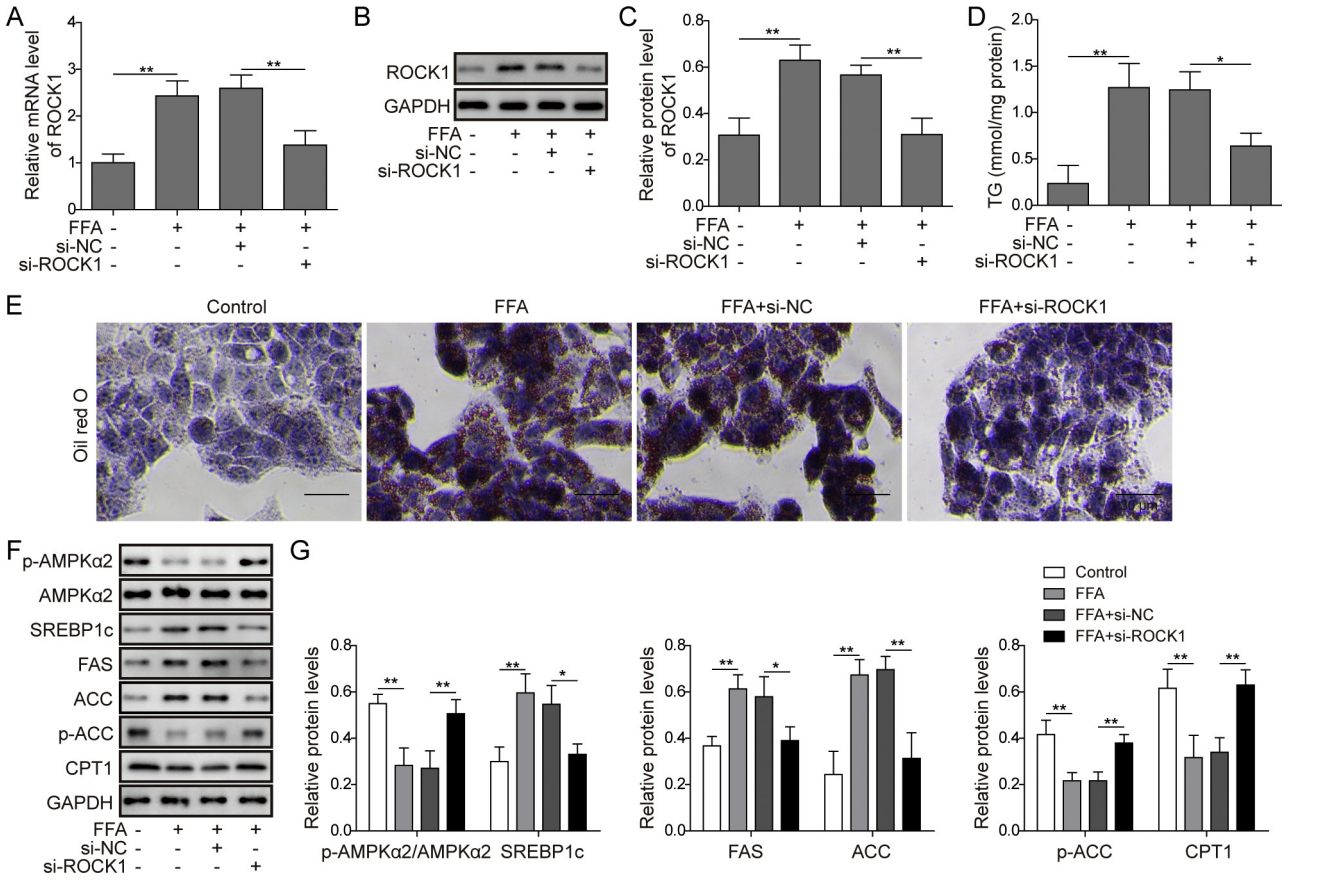

Fig. 5. Silence of ROCK1 alleviated lipid formation induced by FFA. (A–C) The protein and mRNA level of ROCK1 in HepG2 cells transfected with si-ROCK1. (D) The TG level in HepG2 cells transfected with si-ROCK1. (E) Lipid accumulation in HepG2 cells transfected with si-ROCK1 identified by Oil Red O staining. (F–G) The protein levels of AMPK/SREBP signaling pathway-related protein were measured by Western blotting in HepG2 cells transfected with si-ROCK1. Data were shown as the mean ± SD. Each experiment was repeated three times. $^{*}P < 0.05$, $^{**}P < 0.01$.

with no RT and no template control included. Data were analyzed by comparing cycle threshold values.

2.11. Western blotting

Total protein in cells was prepared using lysis buffer. Equal amounts of sample were loaded on an SDS-PAGE and then transferred electrophoretically to PVDF membrane (Millipore, USA). After blocking with TBST (5% non-fat milk), the membranes were incubated overnight with primary antibody (1:800) at 4 °C. Primary antibodies used in this study were listed as follows. Anti-ROCK1 antibody (ab45171, Abcam, UK); Anti-p-AMPKa2 antibody (ab109402, Abcam, UK); Anti-AMPKa2 antibody (ab109402, Abcam, UK); Anti-SREBP1c antibody (ab133125, Abcam, UK); Anti-FAS antibody (ab22759, Abcam, UK); Anti-ACC mouse antibody (3662S, Cell Signaling, Danvers, MA, US). After washing and incubation, the membranes were incubated with secondary antibody (1:1500) in TBST. Immunodetection was achieved using ECL Plus detection system (Millipore, USA). The density of the bands was measured using Image J software.

2.12. Statistical analysis

Assays were performed at least in three independent experiments with one representative picture presented. Data were shown as mean ± standard deviation (SD). Statistical analysis was conducted with SPSS 24.0. Two-tailed student's *t*-test was applied to assess the statistical significance of difference between two independent groups. ANOVA was used for multiple comparison. $P < 0.05$ was considered as statistically significant difference.

3. Result

3.1. NEAT1 and ROCK1 are up-regulated and miR-146a-5p is down-regulated in NAFLD models

To explore the mechanism of lipid accumulation in NAFLD, we established NAFLD models in vivo and in vitro by HFD and FFA treatment, respectively. The relative expression levels of NEAT1, miR-146a-5p and ROCK1 were detected. We found that the expressions level of NEAT1 and ROCK1 were significantly higher in NAFLD models, while the level of miR-146a-5p was significantly lower compared with control group (Fig. 1A and I). The protein expression of ROCK1 was also detected, and significant higher expression of ROCK1 was in line with the result in mRNA level (Fig. 1B and J). The serum TC, TG, AST, and ALT levels were increased remarkably in mice treated by HFD compared with control group (Fig. 1C & D). Hepatic steatosis was presented by HE staining and lipid over-accumulation in the liver of HFD mice was observed via Oil Red O staining (Fig. 1E). HFD treatment markedly increased NAFLD activity score (Fig. 1F). Meanwhile the TG content and the lipid droplets in the HepG2 cells were measured in the HepG2 cells. We found that FFA markedly increased lipid over-accumulation (Fig. 1G) and the content of TG (Fig. 1H) in the HepG2 cells. These findings indicated that NEAT1, miR-146a-5p and ROCK1 might play important roles in regulating NAFLD.

3.2. NEAT1 promotes the expression of ROCK1 via sponging miR-146a-5p

NEAT1 was knocked down in HepG2 cells by transfecting sh-NEAT1. miR-146a-5p was remarkably increased, but ROCK1 was

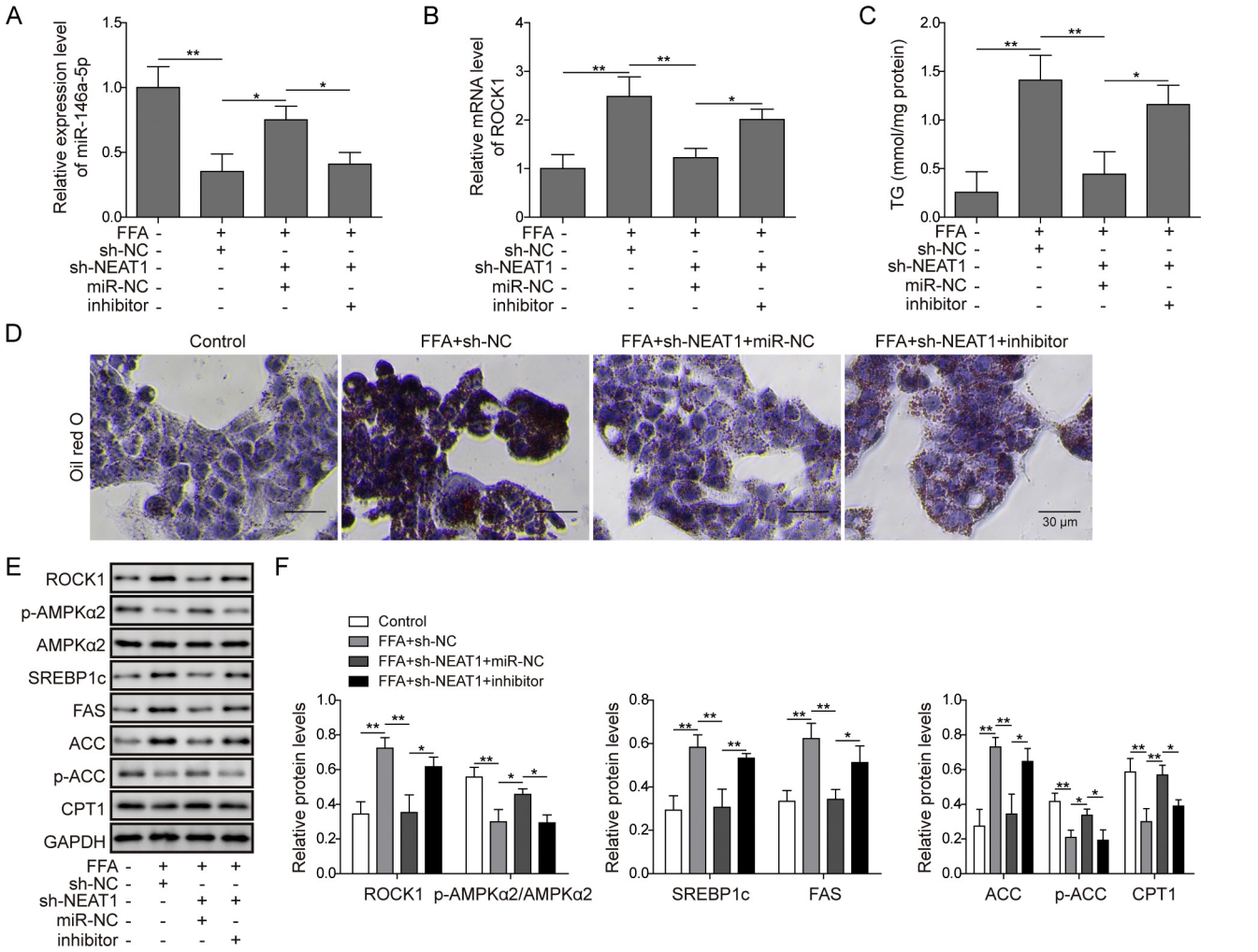

Fig. 6. NEAT1 promoted steatosis through down-regulating miR-146a-5p. (A) The relative level of miR-146a-5p in HepG2 cells after sh-NEAT1 transfection and/or miR-146a-5p inhibitor transfection. (B) The mRNA level of ROCK1 in HepG2 cells after sh-NEAT1 transfection and/or miR-146a-5p inhibitor transfection. (C) TG content in HepG2 cells after sh-NEAT1 transfection and/or miR-146a-5p inhibitor transfection. (D) Lipid accumulation in HepG2 cells after sh-NEAT1 transfection and/or miR-146a-5p inhibitor transfection identified by Oil Red O staining. (E–F) The protein expressions of ROCK1 and AMPK/SREBP signaling pathway-related protein were measured by Western blotting in HepG2 cells after sh-NEAT1 transfection and/or miR-146a-5p inhibitor transfection. Data were shown as the mean ± SD. Each experiment was repeated three times. $^{*}P < 0.05$, $^{**}P < 0.01$.

observably decreased (Fig. 2A). These results suggested that NEAT1 could inhibit miR-146a-5p and promote ROCK1 expression. Then we transfected miR-146a-5p mimics or inhibitor in HepG2 cells, and the ROCK1 level was measured by qRT-PCR. miR-146a-5p mimics could repress ROCK1 expression and miR-146a-5p inhibitor could enhance ROCK1 expression (Fig. 2B). The si-ROCK1 and pcDNA-ROCK1 were also synthesized (Fig. 2C). Next, we found that NEAT1 and 3′-UTR of ROCK1 have potential binding site of miR-146a-5p through bioinformatics method (Fig. 2D–E). Dual luciferase reporter gene assay showed that miR-146a-5p mimics markedly inhibited the luciferase activity of the reporter gene of NEAT1-WT compared with miR-NC group, but brought no influence on NEAT1-MUT (Fig. 2F). Also, only WT-ROCK1 luciferase activity was inhibited by miR-146a-5p mimics (Fig. 2G). These findings indicated that NEAT1 could promote the expression of ROCK1 via sponging miR-146a-5p.

3.3. Down-regulation of NEAT1 remits lipid formation

NEAT1 was significantly increased in HepG2 cells treated with FFA, transfection with sh-NEAT1 significantly reversed the increased NEAT1 in cells induced by FFA (Fig. 3A). Meanwhile, transfection with sh-NEAT1 remarkably increased the level of miR-146a-5p (Fig. 3B), and decreased both mRNA and protein expression of ROCK1 (Fig. 3C–E). Additionally, we measured the effects of NEAT1 and miR-146a on FFA uptake using BODIPY-labeled fatty acid uptake assay. The results showed that knocking down NEAT1 could inhibit FFA uptake by hepatocytes (Fig. 3F) and decrease the expression level of CD36, the key enzyme of fatty acid transmembrane transport (Fig. 3G). Additionally, significant lower TG content in cell (Fig. 3H) and less lipid accumulation (Fig. 3I) were observed after transfecting sh-NEAT1. Then, we measured the expression of AMPK/SREBP signaling pathway-related proteins. FFA treatment significantly inhibited the expression of p-AMPK, p-ACC and CPT1, and increased the expression of SREBP1c, FAS, and ACC (Fig. 3J–K). However, transfection with sh-NEAT1 reversed the influence of FFA, and remarkably increased the expression of p-AMPK, p-ACC and CPT1, and decreased the expression of SREBP1c, FAS, and ACC (Fig. 3J–K). Therefore, knockdown of NEAT1 could promote FFA β-oxidation and alleviate lipid formation by activating AMPK signaling pathway.

3.4. Overexpression of miR-146a-5p moderates lipid deposition caused by FFA

miR-146a-5p was significantly decreased in HepG2 cells treated by

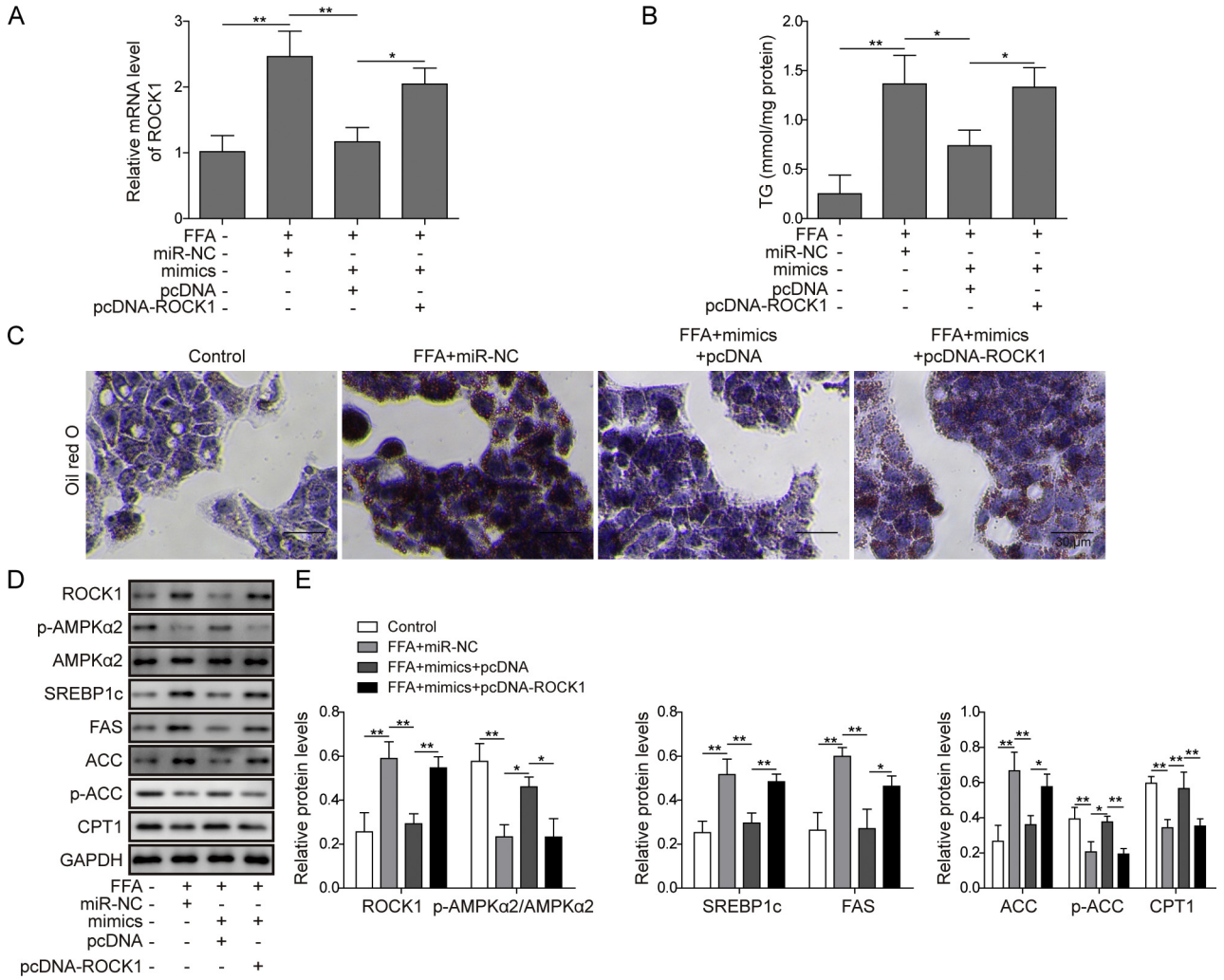

Fig. 7. miR-146a-5p inhibited fatty degeneration by suppressing ROCK1. (A) The mRNA level of ROCK1 in HepG2 cells after miR-146a-5p mimics transfection and/or pcDNA-ROCK1 transfection. (B) TG content in HepG2 cells after miR-146a-5p mimics transfection and/or pcDNA-ROCK1 transfection. (C) Lipid accumulation in HepG2 cells after miR-146a-5p mimics transfection and/or pcDNA-ROCK1 transfection identified by Oil Red O staining. (D-E) The protein expressions of ROCK1 and AMPK/SREBP signaling pathway-related protein were measured by Western blotting in HepG2 cells after miR-146a-5p mimics transfection and/or pcDNA-ROCK1 transfection. Data were shown as the mean ± SD. Each experiment was repeated three times. $^{*}P < 0.05$, $^{**}P < 0.01$.

FFA, transfection with miR-146a-5p mimics remarkably reversed the decreased level of miR-146a-5p in cells caused by FFA (Fig. 4A). Meanwhile, transfection with miR-146a-5p mimics remarkably decreased both the protein and mRNA levels of ROCK1 (Fig. 4B–D) compared with FFA treatment only. Overexpression of miR-146a-5p could inhibit FFA uptake by hepatocytes and decrease the expression level of CD36 (Fig. 4E & F). Additionally, significant lower TG content in HepG2 cells (Fig. 4G) and less lipid accumulation (Fig. 4H) were observed after transfecting miR-146a-5p mimics. Meanwhile, transfection with miR-146a-5p mimics markedly reversed the influence of FFA on AMPK/SREBP signaling pathway, and remarkably increased the expression of p-AMPK, p-ACC and CPT1, decreased the expression of SREBP1c, FAS, and ACC (Fig. 4I–J).

3.5. Silence of ROCK1 alleviates lipid formation induced by FFA

ROCK1 was significantly up-regulated in HepG2 cells treated by FFA, transfection with si-ROCK1 markedly reversed the increased expression of ROCK1 in the cells induced by FFA (Fig. 5A–C). Meanwhile, significant lower TG content (Fig. 5D) and less lipid accumulation (Fig. 5E) were found in HepG2 cells after transfecting si-ROCK1. Transfection with si-ROCK1 also markedly reversed the influence of FFA on AMPK/SREBP signaling pathway, and remarkably increased the expression of p-AMPK, p-ACC and CPT1, and decreased the expression of SREBP1c, FAS, and ACC (Fig. 5F–G).

3.6. NEAT1 accelerates steatosis through down-regulating miR-146a-5p

In order to unfold the regulatory relationship between NEAT1 and miR-146a-5p in NAFLD, NEAT1 and miR-146a-5p were knockdowned simultaneously. We found that FFA could significantly decrease the level of miR-146a-5p (Fig. 6A), and increase the level of ROCK1 (Fig. 6B) and TG content (Fig. 6C) in HepG2 cells. The influence of FFA was remarkably reversed after transfecting sh-NEAT1, but the reversing function by sh-NEAT1 could be inhibited by treatment with sh-NEAT1 and miR-146a-5p inhibitor simultaneously (Fig. 6A–C). Meanwhile, the results of Oil Red O staining also proved the findings described above. FFA significantly increased the lipid over-accumulation, but transfection with sh-NEAT1 reversed that trend, and treatment with sh-NEAT1 and miR-146a-5p inhibitor simultaneously could increase the lipid accumulation compared with treatment with sh-NEAT1 only (Fig. 6D). The influence of NEAT1 and miR-146a-5p on AMPK/SREBP signaling pathway was also investigated by measuring the protein expression of key molecules. The findings indicated that treatment with sh-NEAT1

and miR-146a-5p inhibitor simultaneously could significantly decrease the expression of p-AMPK, p-ACC and CPT1, and up-regulate the protein expressions of ROCK1, SREBP1c, FAS, ACC compared with transfecting sh-NEAT1 only (Fig. 6E–F).

3.7. miR-146a-5p inhibits fatty degeneration by inhibiting ROCK1

We also observed the influence of miR-146a-5p and ROCK1 on TG content in cells and AMPK/SREBP signaling pathway by overexpressing miR-146a-5p and ROCK1 simultaneously. Transfection with miR-146a-5p mimics could significantly inhibit the increase of ROCK1 (Fig. 7A), TG (Fig. 7B), and lipid accumulation (Fig. 7C) induced by FFA. However, this inhibition could be compromised by transfecting pcDNA-ROCK1 simultaneously (Fig. 7A–C). The influence of miR-146a-5p and ROCK1 on AMPK/SREBP signaling pathway was also investigated by measuring the protein expression of key molecules. The results indicated that treatment with miR-146a-5p mimics and pcDNA-ROCK1 simultaneously could significantly decrease the expression of p-AMPK, p-ACC and CPT1, and up-regulate the protein expressions of ROCK1, SREBP1c, FAS, ACC compared with transfecting miR-146a-5p mimics only (Fig. 7D-E).

4. Discussion

NAFLD is closely related with complex metabolic mechanism characterized with free cholesterol and cumulating triglycerides in the liver leading to chronic liver disease. It is believed as the hepatic manifestation of metabolic syndrome ranging from fatty liver to the severe nonalcoholic steatohepatitis, which is a growing risk for cardiovascular disease and diabetes [4,28]. However, the specific molecular pathogenesis of NAFLD remains unknown. Meanwhile, apart from lifestyle alteration, dietary changes and bariatric surgery, no effective medical therapeutics could reverse NAFLD completely [5]. Therefore, investigating underlying mechanism and exploring therapeutic strategies for NAFLD seem meaningful.

LncRNA is a group of RNA transcripts longer than 200 bases, and unable to code protein. However, increasing number of lncRNAs has been identified to be related with diseases including endocrine physiology, obesity, cardiac disorder, neuron disease, and cancer. NEAT1 was significantly up-regulated during adipogenesis especially [29]. Knockdown of NEAT1 decreased the expression of ACC and FAS and alleviated NAFLD progress of rats via repressing mTOR/S6K1 signaling pathway [11]. NEAT1 was reported to promote steatosis via enhancement of estrogen receptor alpha-mediated AQP7 expression in HepG2 cells [13]. Additionally, ROCK1 could regulate insulin resistance, adiposity, and hepatic lipid accumulation [20,21]. However, the underlying mechanism of NEAT1 and ROCK1 in NAFLD is not clear. We found that the expressions of both NEAT1 and ROCK1 were up-regulated in mice and cell models of NAFLD. These findings indicated that both NEAT1 and ROCK1 might play a key role in the pathological processes of NAFLD.

Regulatory function between noncoding RNAs within cell may be involved in the development of some diseases. Competitive endogenous lncRNAs is known as a mechanism of miRNA-lncRNA interaction. For example, lncRNA-regulator of reprogramming (RoR) contains some binding sites targeting specific miRNAs, and lncRNA-RoR could regulate the expression of miRNAs through functioning as a competitive sponge [15]. Meanwhile, miRNAs can also modulate lncRNAs through RNA-induced silencing complex [30]. miR-146a-5p was demonstrated to regulate nonalcoholic fibrosing steatohepatitis by inhibiting the proliferation and activation of hepatic stellate cells through targeting Wnt signaling pathway [17]. However, the regulatory relationship between miR-146a-5p, NEAT1, and ROCK1 has not been fully clarified. In the present study, knockdown of NEAT1 could up-regulate miR-146a-5p, down-regulate ROCK1, and alleviated NAFLD. NEAT1 promoted the expression of ROCK1 through sponging miR-146a-5p. Therefore, regulation of ROCK1 and miR-146a-5p by NEAT1 should be necessary for progression of NAFLD, and NEAT1 might exert the regulation through competitive endogenous mechanism.

AMPK/SREBP pathway and its downstream proteins including FAS and ACC were closely related with lipid metabolism [7,31,32]. Meanwhile, AMPK plays a vital role for ROCK1-mediated lipogenesis as a downstream regulator of ROCK1 [1]. AMPK can regulate energy balance as an intracellular fuel sensor, and SREBP1c can modulate lipogenic processes through activating genes related with triglyceride biosynthesis and fatty acid. Meanwhile, AMPK could alleviate atherosclerosis and hepatic steatosis through inactivating SEREBP1c [7]. Both FAS and ACC take part in the synthesis of lipid, and the aberrant expressions of them are closely involved in NAFLD [11]. However, whether NEAT1 regulates lipid metabolism through AMPK/SREBP pathway remains unclear. In this study, knockdown of NEAT1 increased the phosphorylation of APMK, decreased the level of SREBP1c, FAS and ACC, but overexpression of miR-146a-5p or knockdown of ROCK1 could significantly reversed the above changes caused by NEAT1 inhibition. These results fully demonstrated that NEAT1 may regulate lipid accumulation of NAFLD through miR-146a-5p targeting ROCK1, and further influence AMPK/SREBP pathway.

In conclusion, NEAT1 could promote NAFLD progress through inhibiting miR-146a-5p, up-regulating ROCK1 and facilitating hepatic lipid accumulation. Our study provides a novel insight into the molecular of NAFLD, and lncRNA NEAT1 may serve as a potential target for NAFLD.

Abbreviations

NAFLD	nonalcoholic fatty liver disease
NEAT1	nuclear enriched abundant transcript 1
miR-146a-5p	microRNA-146a-5p
miR-140	microRNA-140
ROCK1	Rho-kinase1
lncRNAs	long noncoding RNAs
HepG2	human hepatocellular carcinoma
FBS	fetal bovine serum
DMEM	Dulbecco's Modified Eagle's Medium
FFA	free fatty acids
CD	chow diet
HFD	high-fat diet
HE	hematoxylin and eosin
ALT	aminotransferase
AST	aspartate aminotransferase
TG	triglyceride
TC	total cholesterol
FAS	fatty acid synthase
ACC	acetyl-CoA carboxylase

Funding

This work was supported by Hunan Natural Science Foundation (No.2019JJ50897).

Declaration of competing interest

The authors declare that there are no conflicts of interest.

References

[1] H. Huang, et al., Rho-kinase/AMPK axis regulates hepatic lipogenesis during overnutrition, J. Clin. Invest. 128 (12) (2018) 5335–5350.
[2] F.S. Wang, et al., The global burden of liver disease: the major impact of China, Hepatology 60 (6) (2014) 2099–2108.
[3] N. Toshikuni, M. Tsutsumi, T. Arisawa, Clinical differences between alcoholic liver disease and nonalcoholic fatty liver disease, World J. Gastroenterol. 20 (26) (2014) 8393–8406.

[4] H. Yki-Jarvinen, Non-alcoholic fatty liver disease as a cause and a consequence of metabolic syndrome, Lancet Diabetes Endocrinol. 2 (11) (2014) 901–910.
[5] A. Iacono, et al., Probiotics as an emerging therapeutic strategy to treat NAFLD: focus on molecular and biochemical mechanisms, J. Nutr. Biochem. 22 (8) (2011) 699–711.
[6] A.L. Birkenfeld, G.I. Shulman, Nonalcoholic fatty liver disease, hepatic insulin resistance, and type 2 diabetes, Hepatology 59 (2) (2014) 713–723.
[7] H. Yao, et al., Dioscin alleviates non-alcoholic fatty liver disease through adjusting lipid metabolism via SIRT1/AMPK signaling pathway, Pharmacol. Res. 131 (2018) 51–60.
[8] Y. Mang, et al., Long noncoding RNA NEAT1 promotes cell proliferation and invasion by regulating hnRNP A2 expression in hepatocellular carcinoma cells, Onco. Targets Ther. 10 (2017) 1003–1016.
[9] M.T. Melissari, P. Grote, Roles for long non-coding RNAs in physiology and disease, Pflugers Arch. 468 (6) (2016) 945–958.
[10] X. Yuan, et al., Berberine ameliorates nonalcoholic fatty liver disease by a global modulation of hepatic mRNA and lncRNA expression profiles, J. Transl. Med. 13 (2015) 24.
[11] X. Wang, Down-regulation of lncRNA-NEAT1 alleviated the non-alcoholic fatty liver disease via mTOR/S6K1 signaling pathway, J. Cell. Biochem. 119 (2) (2018) 1567–1574.
[12] C.M. Clemson, et al., An architectural role for a nuclear noncoding RNA: NEAT1 RNA is essential for the structure of paraspeckles, Mol. Cell 33 (6) (2009) 717–726.
[13] X. Fu, et al., Long non-coding RNA NEAT1 promotes steatosis via enhancement of estrogen receptor alpha-mediated AQP7 expression in HepG2 cells, Artif. Cells Nanomed. Biotechnol. 47 (1) (2019) 1782–1787.
[14] R. Garzon, G.A. Calin, C.M. Croce, MicroRNAs in cancer, Annu. Rev. Med. 60 (2009) 167–179.
[15] R. Gernapudi, et al., MicroRNA 140 promotes expression of long noncoding RNA NEAT1 in adipogenesis, Mol. Cell. Biol. 36 (1) (2016) 30–38.
[16] B.P. Lewis, C.B. Burge, D.P. Bartel, Conserved seed pairing, often flanked by adenosines, indicates that thousands of human genes are microRNA targets, Cell 120 (1) (2005) 15–20.
[17] J. Du, et al., MiR-146a-5p suppresses activation and proliferation of hepatic stellate cells in nonalcoholic fibrosing steatohepatitis through directly targeting Wnt1 and Wnt5a, Sci. Rep. 5 (2015) 16163.
[18] J. Latorre, et al., Decreased lipid metabolism but increased FA biosynthesis are coupled with changes in liver microRNAs in obese subjects with NAFLD, Int. J. Obes. 41 (4) (2017) 620–630.
[19] M. Kajikawa, et al., Rho-associated kinase activity is a predictor of cardiovascular outcomes, Hypertension 63 (4) (2014) 856–864.
[20] S.H. Lee, et al., ROCK1 isoform-specific deletion reveals a role for diet-induced insulin resistance, Am. J. Physiol. Endocrinol. Metab. 306 (3) (2014) E332–E343.
[21] B. Xu, et al., Hsa-miR-146a-5p modulates androgen-independent prostate cancer cells apoptosis by targeting ROCK1, Prostate 75 (16) (2015) 1896–1903.
[22] H.N. Wang, et al., Inhibition of hepatic interleukin-18 production by rosiglitazone in a rat model of nonalcoholic fatty liver disease, World J. Gastroenterol. 14 (47) (2008) 7240–7246.
[23] J. Cai, X.J. Zhang, H. Li, Progress and challenges in the prevention and control of nonalcoholic fatty liver disease, Med. Res. Rev. 39 (1) (2019) 328–348.
[24] A.R. Im, et al., Water extract of Dolichos lablab attenuates hepatic lipid accumulation in a cellular nonalcoholic fatty liver disease model, J. Med. Food 19 (5) (2016) 495–503.
[25] Y. Cheng, et al., Structural shifts of gut flora in rat acute alcoholic liver injury and jianpi huoxue decoction's effect displayed by ERIC-PCR fingerprint, Chin. J. Integr. Med. 17 (5) (2011) 361–368.
[26] W. Choi, et al., Serotonin signals through a gut-liver axis to regulate hepatic steatosis, Nat. Commun. 9 (1) (2018) 4824.
[27] S. Xu, et al., Evaluation of foam cell formation in cultured macrophages: an improved method with Oil Red O staining and DiI-oxLDL uptake, Cytotechnology 62 (5) (2010) 473–481.
[28] Y.H. Zhang, et al., S100A4 gene is crucial for methionine-choline-deficient diet-induced non-alcoholic fatty liver disease in mice, Yonsei Med. J. 59 (9) (2018) 1064–1071.
[29] L. Sun, et al., Long noncoding RNAs regulate adipogenesis, Proc. Natl. Acad. Sci. U. S. A. 110 (9) (2013) 3387–3392.
[30] H. Liang, et al., Nuclear microRNAs and their unconventional role in regulating non-coding RNAs, Protein Cell 4 (5) (2013) 325–330.
[31] N. Higuchi, et al., Liver X receptor in cooperation with SREBP-1c is a major lipid synthesis regulator in nonalcoholic fatty liver disease, Hepatol. Res. 38 (11) (2008) 1122–1129.
[32] S. Ugi, et al., Membrane localization of protein-tyrosine phosphatase 1B is essential for its activation of sterol regulatory element-binding protein-1 gene expression and consequent hypertriglyceridaemia, J. Biochem. 146 (4) (2009) 541–547.